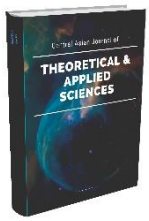


# CENTRAL ASIAN JOURNAL OF THEORETICAL AND APPLIED SCIENCES

**Volume: 03 Issue: 07 | Jul 2022 ISSN: 2660-5317**
**https://cajotas.centralasianstudies.org**


# Size Effects in Mn-DOPED SmFeO3 for Spintronics Applications


**A. K. Singh**
Research Scholar, Department of Physics, Integral University, Dashauli, Kursi Road, Lucknow-226026, UP, India

**S. Srivastava**
Supervisor, Professor, Head of the Department of Physics, Integral University, Dashauli, Kursi Road, Lucknow-226026, UP, India

**V. S. Chandel**
Co-supervisor, Department of Applied Science & Humanities, Rajkiya Engineering College, Ambedkar Nagar-224122, UP, India



*Received 24th May 2022, Accepted 13th Jun 2022, Online 9th Jul 2022*



***Abstract:*** *The intriguing physical properties of SmFeO3 such as spin-phonon coupling and spin reorientation transition (~480 K) make it interesting from fundamental point of view and a suitable candidate for oxide-based spintronic applications. Here, we have studied the temperature dependent structural, vibrational, and magnetic properties of polycrystalline Sm0.9Bi0.1Fe0.9Mn0.1O3 prepared by conventional solid-state reaction method. The compound stabilizes in orthorhombic structure with space group "Pnma" and exhibits no structural phase transitions in the investigated temperature range (300–500 K). Magnetic measurements reveal the weak ferromagnetic–paramagnetic transition at 620 K. Thermal evolution of phonon modes investigated using Raman spectroscopy in the temperature range 300–800 K reveal that Ag(3) phonon mode related to FeO6 vibrations exhibits anomalous behaviour below magnetic transition temperature, which we attribute to spin-phonon coupling. The optical band gap value of ∼5.17 eV has been estimated from the analysis of UV‑Vis diffuse reflectance spectroscopy using the Tauc relation. The value of Δ Et2u→t2g is estimated to be ~ 2.6 eV for p-d charge transfer transitions in Fe/MnO6 octahedra. The obtained valence states from X-ray photoelectron spectroscopy analysis of all the elements of the sample are in excellent agreement with the expected values.*



***Keywords:*** *size, effects, spin, doping, coupling, spintronics, Mn-doped, SmFeO3.*


## Introduction

The XRD pattern analysis shows that all the peaks for $SmFe_{1-x}Cr_xO_3$ samples can be indexed according to the crystal structure of pure $SmFeO_3$ and has a fine crystal structure. The dielectric constants of $SmFe_{1-x}Cr_xO_3$ (x = 0.1–0.3) ceramics ($\varepsilon_r$ = 2532, 1959, 1172) are only 0.86, 0.67 and 0.41 times that of $SmFeO_3$ ($\varepsilon_r$ = 2914) at 1 kHz, respectively.

The change of dielectric constant ($\varepsilon_r$) with x is mainly the result of the internal barrier layer capacitor (IBLC) mechanism and the dipole oriented polarization mechanism. It shows that the M-H of $SmFeO_3$ at room temperature exhibits a butterfly shape disappears with the increase of $Cr^{3+}$ and the magnetic properties is also gradually weakened, indicating that $Cr^{3+}$ doping can effectively regulate the M-H of $SmFeO_3$. On the M-T curve, it is found that the $T_{SR}$ and $T_N$ of SFO decrease from 462 K to 687 K–428 K .[1,2]

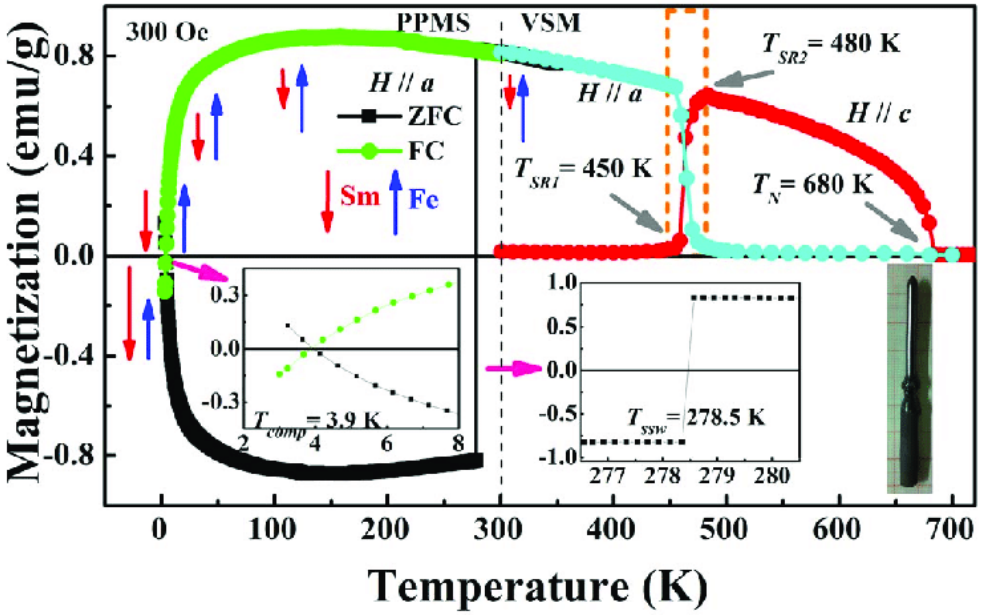


Uniform perovskite type SmFeO3 and SmCoO3 nanofibers have been prepared by a simple electrospinning approach and calcination process. The obtained samples had orthorhombic structure and strong absorbance behaviors in UV-vis regions. The diameters of SmFeO3 and SmCoO3 nanofibers were 220 and 300 nm, respectively. The electrochemical and magnetic properties of SmFeO3 and SmCoO3 were investigated. SmFeO3 and SmCoO3 electrodes exhibited typical pseudocapacitive behaviors owing to the redox reactions of Fe3+/Fe2+ and Co3+/Co2+. At 0.5 A g-1, the specific capacitances of SmFeO3 and SmCoO3 nanofibers were 90.8 and 126.6 F g-1, respectively.[3,4] The high-performance nanostructured SmFeO3 and SmCoO3 have significantly potential application in supercapacitors. SmFeO3 nanofibers exhibited weak ferromagnetic behavior. SmCoO3 nanofibers presented paramagnetism at high temperature and ferromagnetism at 5 K.[5,6]

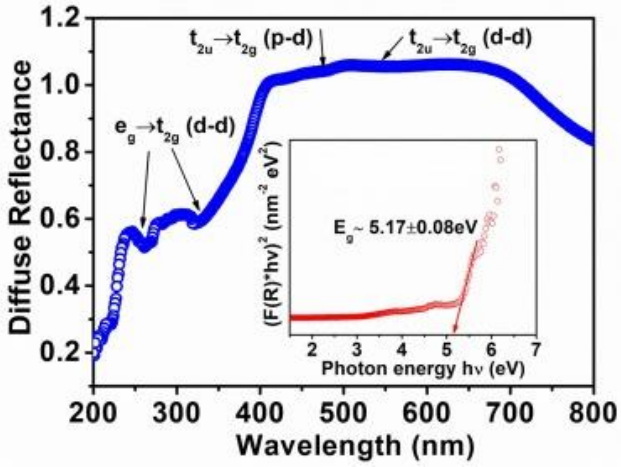


 

We perform first principles simulations for the structural, elastic, vibrational, electronic and optical properties of orthorhombic samarium orthoferrite $SmFeO_3$ within the framework of density functional theory. A number of different density functionals, such as local density approximation, generalized gradient approximation, Hubbard interaction modified functional, modified Becke-Johnson approximation and Heyd–Scuseria–Ernzerhof hybrid functional have been used to model the exact electron exchange-correlation. We estimate the energy of the ground state for different magnetic configurations of $SmFeO_3$.[7,8]

Its crystal structure is characterized in terms of calculated lattice parameters, atomic positions, relevant ionic radii, bond lengths, bond angles and compared with experimental values. The stability of its orthorhombic structure is simulated in terms of elastic properties. The vibrational phonon modes are calculated using density functional perturbation theory and are shown to be consistent with recent experimental observations. In case of electronic properties, we provide estimates based on density functionals with varying degrees of computational complexities in the Jacob's ladder. We show Heyd–Scuseria–Ernzerhof density functional theory provides better modelling for localized d and f orbitals in SFO which is in line with theoretical work on other rare-earth materials.[9,10]

The linear optical properties in terms of complex dielectric function and other standard optical functions are derived for Hubbard corrected generalized gradient approximation in combination with Fermi's golden rule.These provide a good theoretical analysis of structural, elastic, vibrational, electronic and optical properties of SFO. Temperature-induced multiple magnetic transitions, spin reorientation, spin switching and compensation point, and possible mechanism are investigated in $Sm_{0.5}Pr_{0.5}FeO_3$ single crystal. Compared with $SmFeO_3$, spin reorientation temperature ($T_{SR}$) of $Sm_{0.5}Pr_{0.5}FeO_3$ was effectively modulated from 450 K–480 K to 180 K–220 K. Spin switching temperature ($T_{ssw}$) also decreases from 180 K to 119 K, while compensation point temperature ($T_{comp}$) was raised from 4 K to 90 K. By substituting $Pr^{3+}$ in $SmFeO_3$[11,12]

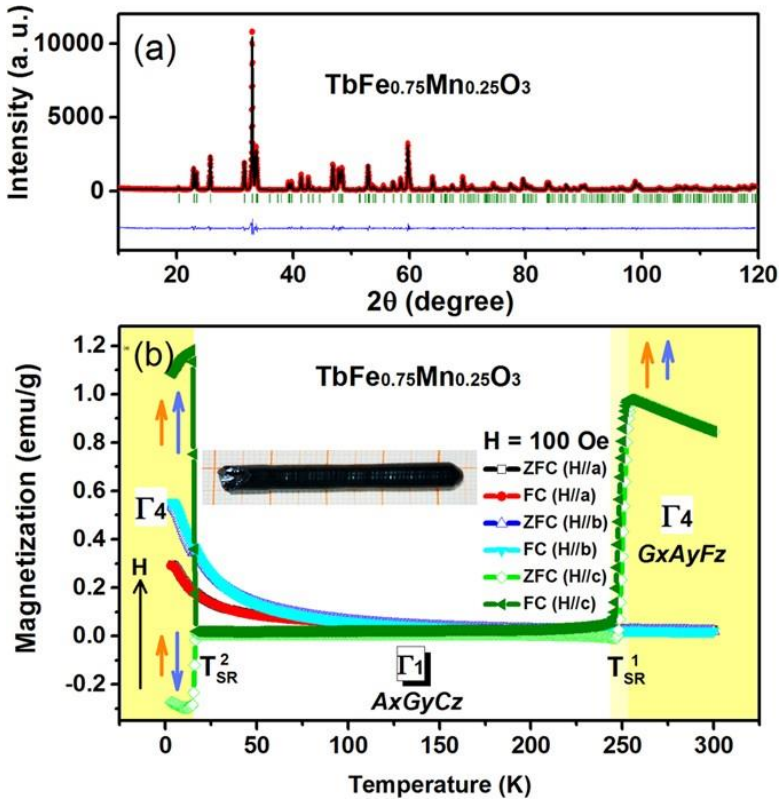


 

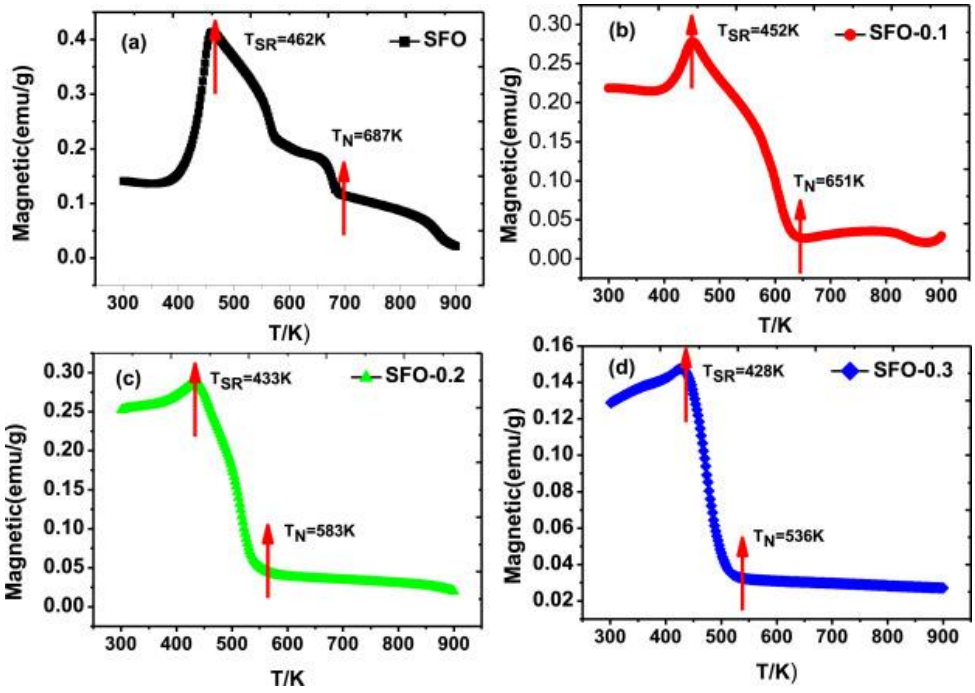


## Discussion

Magnetoelectric (ME) materials composed of magnetostrictive and piezoelectric phases have been the subject of decades of research due to their versatility and unique capability to couple the magnetic and electric properties of the matter. While these materials are often studied from a fundamental point of view, the 4.0 revolution (automation of traditional manufacturing and industrial practices, using modern smart technology) and the Internet of Things (IoT) context allows the perfect conditions for this type of materials being effectively/finally implemented in a variety of advanced applications. Demands for miniaturization, increasing the operation speed and energy efficiency of electronic devices led to the emergence and rapid development of spin electronics, or spintronics.[13,14]

Several areas of experimental and theoretical research are considered, in which the Ioffe Institute is actively involved. We discuss current progress in developing semiconductor and hybrid structures that exhibit specified magnetic properties, the development of methods for manipulating individual spins, a theoretical description of switching of metallic heterostructures magnetization by an electric field, and ultrafast control of magnetization via manipulating the magnetic anisotropy by femtosecond laser pulses.[29,30] Magnetoelectric multiferroic materials provide a unique opportunity to exploit several functionalities in a single material. Therefore, such materials have attracted significant interest due to both potentials in extensive technological applications such as, non-volatile memories and data storage devices, spintronics, consumer electronics, etc. Especially, owing to magnetoelectric coupling those have potential in designing spintronic devices with low power consumption and high storage density [15,16]. Among such materials, Bismuth ferrite, BiFeO3 (BFO), is unique single phase magnetoelectric multiferroic material. Consequently, to enhance magnetic properties, one needs to suppress and collapse the spin cycloid structure. For instance, destruction of spin cycloid structure of ABO3 perovskite type multiferroics such as SmFeO3 by doping and hereby improving magnetic properties were succeeded[17,18]

 

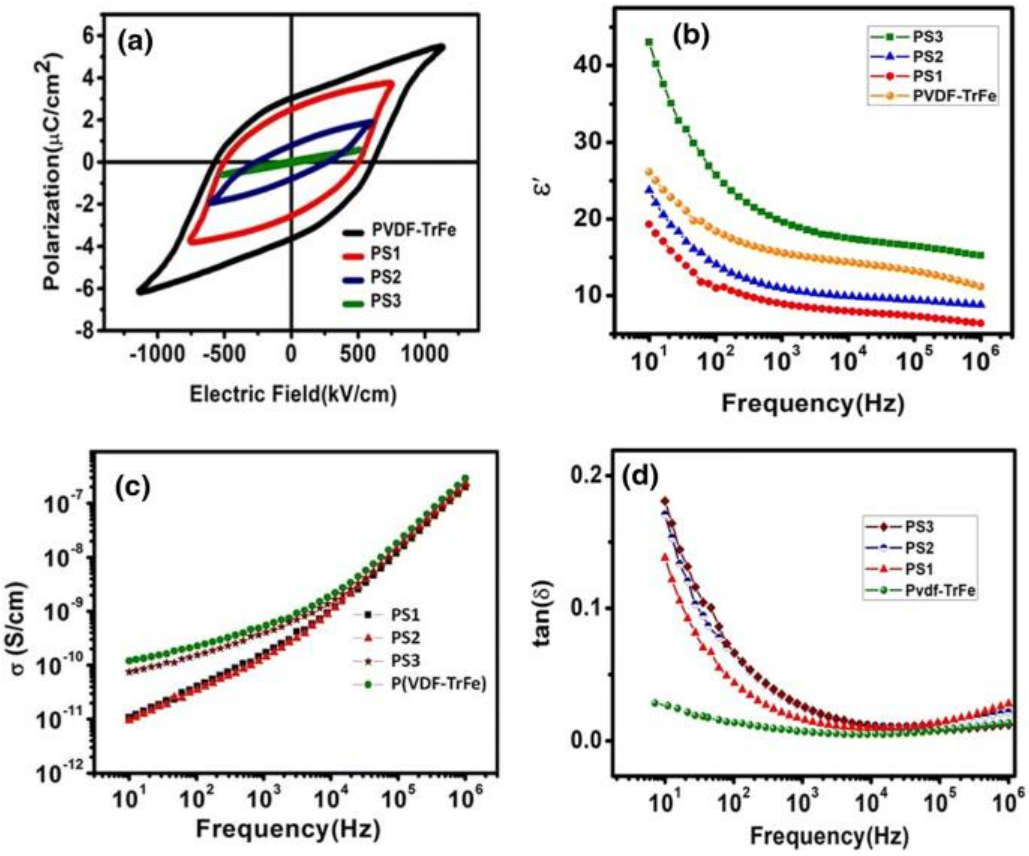


As is well known from the bulk BFO crystal, that the G-type inhomogeneous antiferromagnetic spin order is rotating in a plane parallel to (110)h resulting in an incommensurate modulated spin structure. The magnetization vs. magnetic field (M-H) plot of pure BFO exhibits a near linear relationship due to spin cycloid structure with long period wavelength of ~62 nm. As a consequence, the vector summation of magnetization is averaged to zero remanent magnetization in this period. [27,28]On the contrary, suitable ion substitutions may be able to destruct space-modulated cycloid structure and release latent magnetization with homogenous spin state. The M-H measurements of BFO and BLFGO samples are plotted in Fig. 5. Clearly, the hysteresis curves revealed an enhancement in the magnetic properties upon La and Gd substitutions. Evidently, hysteresis loop of BFO is observed almost linear which is pointing out antiferrerromagnetic spin order, on the other hand, those of BLFGO samples are non-saturated ferromagnetic comparatively well opened with high remanent magnetization and coercivity. [19,20] The shapes of the M-H loops of BLFGO look similar, however, there is substantial enhancement of magnetization value by increasing Gd ratio.

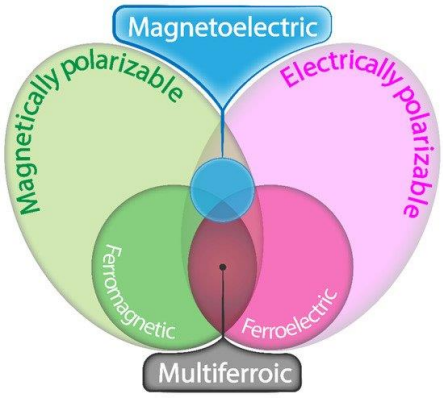


 

## Results and Conclusions

The corresponding magnetic parameters, such as double coercivity (2HC) and remanent magnetization (2Mr), provided with hysteresis loops. [21,22]

The temperature and field dependence of the magnetization of epitaxial, undoped anatase $TiO_2$ thin films on $SrTiO_3$ substrates was investigated. Low-energy ion irradiation was used to modify the surface of the films within a few nanometers, yet with high enough energy to produce oxygen and titanium vacancies.[25,26] The as-prepared thin film shows ferromagnetism which increases after irradiation with low-energy ions. An optimal and clear magnetic anisotropy was observed after the first irradiation, opposite to the expected form anisotropy. Taking into account the experimental parameters, titanium vacancies as di-Frenkel pairs appear to be responsible for the enhanced ferromagnetism and the strong anisotropy observed in our films. The magnetic impurities concentrations was measured by particle-induced X-ray emission with ppm resolution. They are ruled out as a source of the observed ferromagnetism before and after irradiation.[23,24]

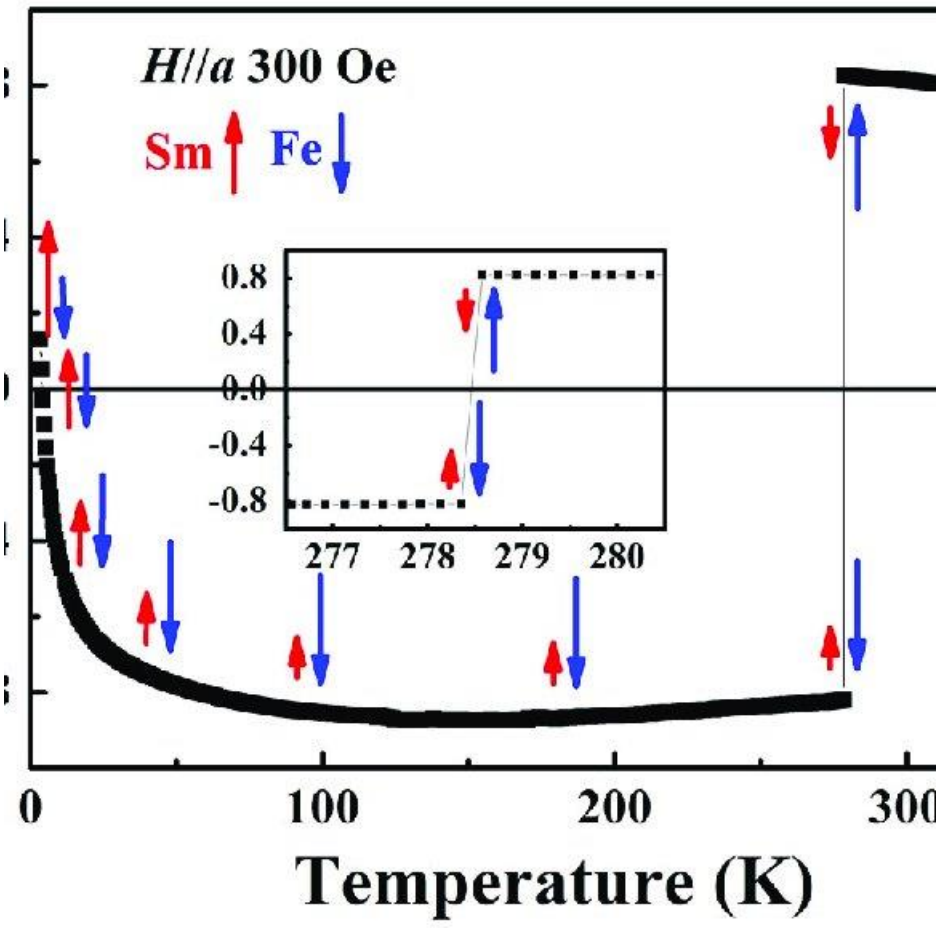


## References

1. C.N.R. Rao, V.G. Bhide, and N.F. Mott. Philos Mag;32, (1975). p.1277.
2. C.N.R. Rao, and O.M. Parkash. Philos. Mag.;35, (1977). p. 1111.
3. A. Casalot, P. Dougieret, and P. Hagenmuller. J PhysChem Solids;32, (1971). p. 407.
4. D.S. Rajoria, V.G. Bhide, G.R. Rama, and C.N.R. Rao. J. Chem. Soc., Faraday Trans; 70, (1973). p. 512.

5. G. Thornton, F.C. Morrison, S. Partington, B.C. Tofield, and D.E. Williams. J Phys C: Solid State Phys.; 21, (1988). p. 2871.
6. Y. Tokura, Y. Okimoto, S. Yamaguchi, H. Taniguchi, T. Kimura, and H. Takagi. Phys. Rev B;58, (1998). p. 1699.
7. T. Lottermoser, T. Lonkai, U. Amann, D. Hohlwein, J. Ihringer, and M. Fiebig. Nature (London); 430, (2004). p. 541.
8. S.W. Cheong, and M. Mostovoy. Nat. Mater;6, (2007). p. 13.
9. T.H. Lin, Shih HC, C.C. Hsieh, Luo CW, J-Y Lin, J.L. Her, H.D. Yang, Hsu CH, K.H. Wu, T.M. Uen, and J.Y. Juang. J Phys: CondensMatter ;21, (2009). p. 026013.
10. S.J. Luo, S.Z. Li, N. Zhang, T. Wei, X.W. Dong, K.F. Wang, and J.M. Liu. Thin Solid Films;519, (2010). p. 240.
11. R. Ramesh, and N.A. Spaldin - Multiferroics: progress and prospects in thin films, Nature materials; 6, (2007). p.21.
12. Y.H. Lee, J.M. and W. Epitaxial Journal of Crystal Growth, 263, (2004). p. 436.
13. J.W. Seo, E.E. Fullerton, F. Nolting, A. Scholl, J. Fompeyrine, and J.P. Locquet . J Phys: Condens. Matter; 20,1 (2008).
14. S. Acharya, P.K. Chakrabarti - Solid State Commun.;150, (2010). p. 1234.
15. N. F. Atta, A. Galal and S. M. Ali, Int. J. Electrochem. Sci., 9, (2014). p. 2132.
16. B. V. Prasad, G. NarsingaRao, J.W. Chen, and D. Suresh Babu, Materials Research Bulletin 46, (2011). p. 1670.
17. M.A. Pena, and J.L.G. Fierro, Chem. Rev. 101, (2001). p. 1981.
18. P. Mandal, C.R. Serrao, E. Suard, V. Caignaert, B. Raveau, A. Sundaresan, and C.N.R. Rao; J. Solid State Chem. 197, (2013). p. 408.
19. A. Tiwari, C. Jin, and J. Narayan, Appl. Phys. Lett. 80, (2002). p. 4039.
20. L. M. Berndt, V. Balbarin, and Y. Suzuki, Appl. Phys. Lett. 77, (2000). p. 2903.
21. M. L. Moreira, E. C. Paris, G. S. Nascimento, V. M. Longo, J. R. Sambrano, V. R. Mastelaro, M. I. B. Bernardi, J. Andr_es, J. A. Varelae, and E. Longo, Acta Mater. 57, (2009). p. 5174.
22. H. Forestier and G. Guilt-Guillain, C. R. Acad. Sci. 230, (1950) p. 1884.
23. D. Treves, Phys. Rev. 125, (1962). p. 1843.
24. M. P. Pasternak, W. M. Xu, G. Kh. Rozenberg, and R. D. Taylor, Mat. Res. Soc. Symp. Proc., D2.7.1 (2002). p. 718.
25. A. Wu, H. Shen, J. Xu, Z. Wang, L. Jiang, L. Luo, S. Yuan, S. Cao, and H. Zhang, Bull. Mater. Sci. 35, (2012). p. 259.
26. T. G. Ho, T. D. Ha, Q. N. Pham, H. T. Giang, T. A. T. Do, and N. T. Nguyen, Adv. Nat. Sci.: Nanosci. Nanotechnol. 2, (2011). p. 015012.
27. S. Geller, J. Chem. Phys. 24, (1956). p. 1236.
28. M. A. Gilleo, J. Chem. Phys. 24, (1956). p. 1239.
29. R. Kumar, R. J. Choudhary, M. Ikram, D. K. Shukla, S. Mollah, P. Thakur, K. H. Chae, B. Angadi, and W. K. Choi, J. Appl. Phys. 102, (2007). p. 073707
30. R. Kumar, R. J. Choudhary, M. W. Khan, J. P. Srivastava, C. W. Bao, H. M. Tsai, J. W. Chiou, K. Asokan, and W. F. Pong, J. Appl. Phys. 97, (2005). p. 093526

 